Dynamical effects of Pauli blocking on resonant multi-electron ionization

D.D. Su[1,2], Y.T. Li[1,2,3], Q. Su[4] and R. Grobe[4]

(1) Beijing National Laboratory for Condensed Matter Physics, Institute of Physics, Chinese Academy of Sciences, 100190 Beijing, China

(2) School of Physical Sciences, University of Chinese Academy of Sciences, 100049 Beijing, China

(3) Songshan Lake Materials Laboratory, 523808 Dongguan, Guangdong, China

(4) Intense Laser Physics Theory Unit and Department of Physics Illinois State University, Normal, IL 61790-4560, USA

We examine the dynamical role of the Pauli exclusion principle on resonant multi-electron ionization. Using a simple essential state model that permits us approximate but analytical solutions, we show that this principle can lead to several unexpected consequences. It has only a transient effect on the resonant multi-electron dynamics and its dynamical impact decreases with increasing Rabi frequency. Due to mutually competing mechanisms, this principle can enhance the ionization probability, while at the same time it also decreases the probability for double ionization. Furthermore, it can also manifest itself in the energy distribution of the ionized electrons, but only if the energy accumulation range of the electronic detector is chosen to be sufficiently wide.

1. Introduction

In 1955, S. Autler and C. Townes examined the effect of a resonant laser field on the dressed energy structure of a multi-level quantum system [1]. It was found that the effective energies of the two resonant states were split into doublets, which were separated by the Rabi frequency associated with the field. This light-induced splitting changed the usual singly peaked fluorescent spectrum of these atoms and molecules into the famous Mollow triplet [2], where the usual central peak is accompanied by two side bands.

In 1978, P.L. Knight [3] showed that this Autler-Townes effect can also lead to a splitting of the kinetic energy of electrons in resonant two-photon photoionization, where the ground state population can decay into the continuum via a resonant intermediate bound state. In 1993, it was suggested by numerical simulations that this coherence effect can also be communicated from one electron to another electron due to electron-electron correlations [4,5]. The coherence associated with resonant oscillations of a deeply bound inner electron can be transferred to the photoelectron spectrum of the loosely bound outer electron. This prediction was also confirmed experimentally in 1995 by L. Di Mauro's group [6] in the two-photon ionization of calcium. The resonant photoionization can also occur in systems of two spatially well-separated atoms, where a stepwise behavior of the ionization probability and a Mollow-type photoelectron spectrum is obtained, as well, when the field intensity is large enough [7,8].

Just recently, it was predicted that this Autler-Townes effect can even be transferred between the created electrons and positrons in the laser field-induced vacuum decay process in the presence of a highly charged nucleus [9]. Here the created electron can be captured subsequently by the binding field of the nucleus. If the nucleus's transition frequency between two of its bare levels matches the laser frequency, the captured electron can perform Rabi oscillations between these two levels. The captured electron's dynamics has an immediate impact on the kinetic energy spectrum of the created positrons. It turns out that its positronic energy distribution can reveal split peaks whose energy separation is given precisely by the Rabi frequency of the captured electron.

In all of these phenomena, the electronic Rabi oscillations affected a second particle, such as the electron or the positron, but the presence of this second particle did not impact the Rabi oscillations of the first electron. While these effects have been extensively studied during the past decades, we will examine for the first time a multi-particle mechanism, where the presence of the second particle directly affects the possibility for Rabi oscillations.

The role of Autler-Townes splitting in attosecond ionization was very recently examined theoretically and also experimentally for autoionizing states in argon [10]. Most recent state-of-the-art calculations of the Autler-Townes effect for specific atoms or molecules [11-15] have naturally incorporated the Pauli exclusion principle with regard to the bare energy level structure, but to the best of our knowledge, the quantitative magnitude of its dynamical relevance has not been investigated yet. There are even rather obvious questions that have not been addressed. For example, it is not known, if this principle increases or decreases the overall stability towards ionization or it affects the single and double ionization processes differently. Are there only transient manifestations of this principle, and if so, on which time scales do they occur?

This work is organized as follows. In Section 2, we briefly review the essential state formalism usually being employed to examine resonant ionization of a single-electron atom or ion. In Section 3, we introduce the analytical framework that will permit us to distinguish between the time-dependence of various observables for two-electron systems with and without the Pauli exclusion principle. In Section 4, we present numerical examples that illustrate how this principle can destabilize the atom by increasing its ionization probability while at the same time it decreases the probability for double ionization. We also point out the unexpected role the detector's energy resolution plays for the ionized electrons. We complete with an outlook on open questions, which might motivate further studies.

2. The underlying single-electron model

In order to be able to capture the basic dynamical features of the Pauli-suppression in resonant two-electron ionization, we purposely examine here the simplest possible model and therefore include only the minimally necessary states and their couplings. As we neglect the impact of the electron-electron correlations on the bare energy level structure, we can assume that one electron is initially in the ground level $|1\rangle$ with energy E_1 and the other electron is in the first excited state level $|2\rangle$ energy E_2. In Figure 1 we have sketched the relevant bare energy levels of this restricted Hilbert space for the corresponding two decoupled single-electron systems together with the relevant one-photon couplings. In the right sketch we display the corresponding two two-electron systems with and without the Pauli exclusion principle. In the absence of any Pauli-exclusion principle, the two-electron dynamics separates into two decoupled single-electron systems.

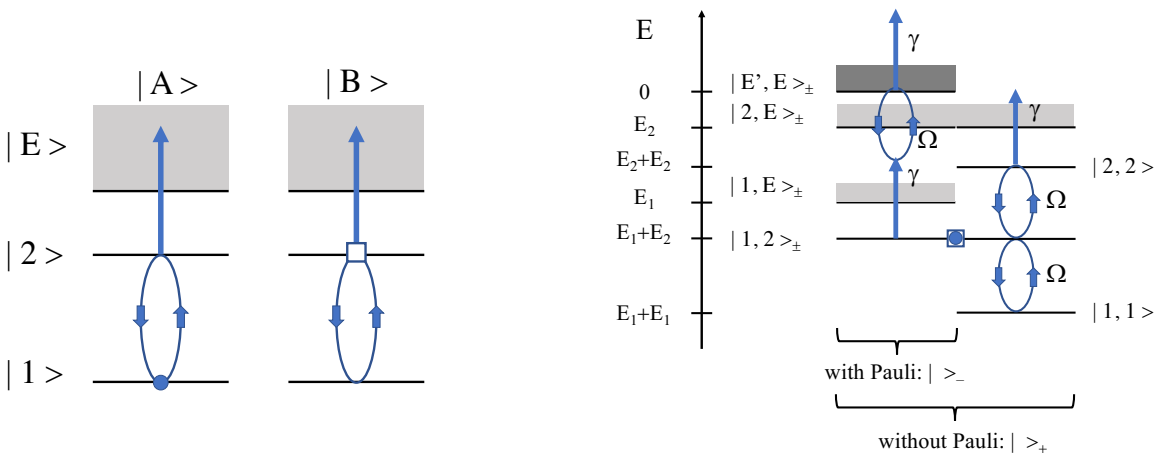

Figure 1 Sketch of the relevant bare energy levels of the two decoupled one electron systems (left) and the two-electron system with and without the Pauli-exclusion principle (right) together with the relevant single-photon couplings. The subscripts ± corresponds to the type of symmetrization used. The relevant energy levels are at $E_1 = -1.5$, $E_2 = -0.5$, $\omega = 1$.

Before we compare the two-particle dynamics with and without the Pauli principle, let us briefly review in this Section the dynamical features of the underlying single-electron system. It is characterized by the state

$$|\phi(t)\rangle = C_1(t)\,|1\rangle + C_2(t)\,|2\rangle + \int dE\, C_E(t)\,|E\rangle \tag{2.1}$$

which is normalized according to $\langle\phi(t)|\phi(t)\rangle = |C_1(t)|^2 + |C_2(t)|^2 + \int dE\,|C_E(t)|^2 = 1$. We assume that the coupling matrix element between the single-particle ground state $|1\rangle$ and the first excited state $|2\rangle$ is given by $\langle 1|H|2\rangle = \Omega(t)$. Here $\Omega(t) \equiv \Omega_0\,\mathrm{Sin}(\omega t)$, where Ω_0 denotes the product of the amplitude of the external oscillatory field with frequency ω and the dipole moment between both discrete states. The corresponding coupling between the first excited state $|2\rangle$ and the continuum state $|E\rangle$ is given by $\langle 2|H|E\rangle = \gamma(t)$, where $\gamma(t) \equiv \gamma\,\mathrm{Sin}(\omega t)$. For simplicity, we assume that the coupling strength γ to any continuum state does not depend on the energy E of the state. The resulting Hamiltonian $H_0 + H_{int}$ takes therefore the form

$$H_0 = E_1\,|1\rangle\langle 1| + E_2\,|2\rangle\langle 2| + \int dE\, E\,|E\rangle\langle E| \tag{2.2a}$$

$$H_{int} = \Omega(t)\,[\,|1\rangle\langle 2| + |2\rangle\langle 1|\,] + \gamma(t)\int dE\,[\,|E\rangle\langle 2| + |2\rangle\langle E|\,] \tag{2.2b}$$

In order to find the equation of motion of the expansion coefficients $C_1(t)$, $C_2(t)$ and $C_E(t)$, we insert the expansion for $|\phi(t)\rangle$ into the Schrödinger equation, given (in atomic units) by $i\, d\, |\phi\rangle /dt= (H_0 + H_{int})\, |\phi\rangle$. If we use the orthogonality among all states, we obtain

$$i\, d\, C_1 / dt \;=\; E_1\, C_1 \;+\; \Omega(t)\, C_2 \tag{2.3a}$$

$$i\, d\, C_2 / dt \;=\; E_2\, C_2 \;+\; \Omega(t)\, C_1 \;+\; \gamma(t) \int dE\, C_E \tag{2.3b}$$

$$i\, d\, C_E / dt \;=\; E\, C_E \;+\; \gamma(t)\, C_2 \tag{2.3c}$$

In order to be able to study the exact predictions from Eqs. (2.3) for arbitrary parameters, one can restrict the upper and lowest energy of the continuum states, assume that they are equidistantly separated by δE and therefore represent the continuum by N_E states. The resulting (N_E+2) equations can then be solved numerically. For sufficiently large N_E and small δE, one can easily obtain fully converged solutions $C_1(t)$, $C_2(t)$ and $C_E(t)$, which are independent of the choice for the computational parameters N_E and δE for all interaction times.

The ionization dynamics is characterized by the relationship of γ, Ω_0, ω to E_1 and E_2. Under the rotating wave approximation, solutions for the time-dependence of the amplitudes can be obtained approximately. We briefly review this standard approach in Appendix A. For the special case of zero detuning, i.e. $E_2 - E_1 = \omega$, the approximate solutions for the two bound states are $\{c_1(t), c_2(t)\} = U(t)\, \{c_1(0), c_2(0)\}$, where the four elements of the 2×2 propagator matrix U(t) are given by

$$U_{1,1}(t) \;=\; \mathrm{Exp}(-t\,\Gamma/4)\, [\, \mathrm{Cos}(\Omega\, t/2) + \Gamma\, \mathrm{Sin}(\Omega\, t/2)/(2\Omega)\,] \tag{2.4a}$$

$$U_{1,2}(t) \;=\; i\, \mathrm{Exp}(-t\,\Gamma/4)\, \Omega_0\, \mathrm{Sin}(\Omega\, t/2)/\Omega \tag{2.4b}$$

$$U_{2,1}(t) \;=\; i\, \mathrm{Exp}(-t\,\Gamma/4)\, \Omega_0\, \mathrm{Sin}(\Omega\, t/2)/\Omega \tag{2.4c}$$

$$U_{2,2}(t) \;=\; \mathrm{Exp}(-t\,\Gamma/4)\, [\, \mathrm{Cos}(\Omega\, t/2) - \Gamma\, \mathrm{Sin}(\Omega\, t/2)/(2\Omega)\,] \tag{2.4d}$$

Here we have introduced the effective Rabi frequency $\Omega \equiv (\Omega_0^2 - (\Gamma/2)^2)^{1/2}$, where in our notation we have assumed $\Omega_0 > \Gamma/2$. The Fermi-Golden rule (FGR) decay rate is given by $\Gamma \equiv 2\pi (\gamma/2)^2$.

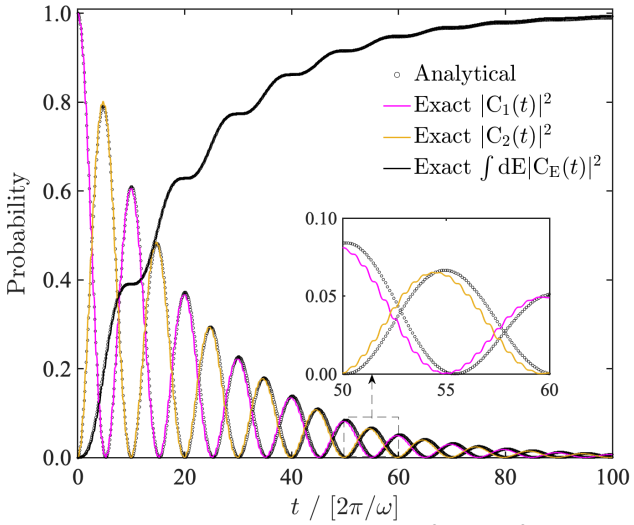

Figure 2 Comparison of the exact probabilities $|C_1(t)|^2$, $|C_2(t)|^2$ and $\int dE\ |C_E(t)|^2$ obtained numerically from Eqs. (2.3) with the approximate but analytical predictions according to $|U_{1,1}(t)|^2$, $|U_{2,1}(t)|^2$ and $1- |U_{1,1}(t)|^2- |U_{2,2}(t)|^2$ and given by Eqs. (2.4). In the inset we show the fast oscillations that the analytical model cannot capture.
[$c_1(0) =1$, $\gamma = 0.15$, $\Omega_0 = 0.1$, $\omega = 1$, $E_1 = -1.5$ and $E_2 = -0.5$. The continuum states were discretized with 200 levels for energies $0.2 < E < 0.8$]. Here the FGR rate amounts to $\Gamma = 0.0353$ and $\Omega = 0.0984$.

In order to test the quality of these approximate expressions for the bound state amplitudes for our parameters studied below, we compare them in Figure 2 with the exact time evolution. We find basically no major differences, suggesting that we can rely on the analytical expressions of Eq. (2.4) for a qualitative analysis in the following Sections. In order to see some discrepancies, in the inset we enlarge the data between the 50th and 60th laser cycle. It reveals that the analytical theory cannot reproduce the superimposed very fast oscillations on the time scale $2\times 2\pi/\omega$ as well as the precise phase of the true signal, as one can expect from the rotating wave approximation.

3. The two-electron models with and without the Pauli-exclusion principle

As we want to focus solely on the dynamical impact of the Pauli-suppression, we neglect here the effect of the electron-electron correlations on any possible shifts to the bare energies. This permits us to exploit the single-particle Hilbert space structure (shown in Figure 1 above) to construct the corresponding space for the two-electron system.

In order to evaluate quantitatively the dynamical impact of the Pauli exclusion principle, we have to compare the predictions with a system where this mechanism is absent. This system for comparison is characterized by the symmetrized two-electron state

$$|\Psi_I(t)\rangle \equiv \left[|A(t)\rangle\,|B(t)\rangle + |B(t)\rangle\,|A(t)\rangle\right]/N^{1/2} \tag{3.1}$$

where $|A(t)\rangle \equiv A_1(t)\,|1\rangle + A_2(t)\,|2\rangle + \int dE\, A_E(t)\,|E\rangle$ and $|B(t)\rangle \equiv B_1(t)\,|1\rangle + B_2(t)\,|2\rangle + \int dE\, B_E(t)\,|E\rangle$ are the corresponding single-electron states satisfying the initial conditions $|A(t=0)\rangle = |1\rangle$ and $|B(t=0)\rangle = |2\rangle$. In order to model the indistinguishability of the two electrons, we have symmetrized the state $|\Psi_I(t)\rangle$ in Eq. (3.1). While for a general symmetrization the normalization factor depends on the relationship among the single particle states, i.e., $N \equiv \langle\Psi_I|\Psi_I\rangle = 2\left[1+|\langle A|B\rangle|^2\right]$, here the factor $N \equiv 2$ reflects the mutual orthogonality of $|A\rangle$ and $|B\rangle$. This orthogonality is maintained at all times as two states are solutions to the same Hamiltonian of Eq. (2.2) and differ only by their initial conditions. This means we have $\langle A(t)|A(t)\rangle = \langle B(t)|B(t)\rangle = |A_1|^2 + |A_2|^2 + \int dE\,|A_E|^2 = |B_1|^2 + |B_2|^2 + \int dE\,|B_E|^2 = 1$ as well as $\langle A(t)|B(t)\rangle = A_1^* B_1 + A_2^* B_2 + \int dE\, A_E^* B_E = 0$.

The six types of time dependent coefficients $A_1(t)$, $A_2(t)$, $A_E(t)$, $B_1(t)$, $B_2(t)$ and $B_E(t)$ are obtained as numerical solutions from Eqs. (2.3) with the initial condition $A_1(0) = 1$, $A_2(0) = A_E(0)=0$ and $B_1(0) = 0$, $B_2(0) = 1$ and $B_E(0) = 0$. In terms of these amplitudes, the state becomes

$$\begin{aligned}|\Psi_I(t)\rangle = \big[&2\,A_1 B_1\,|1\rangle|1\rangle + (A_1 B_2 + B_1 A_2)\,(|1\rangle|2\rangle + |2\rangle|1\rangle) + (A_1 \textstyle\int dE\, B_E + B_1 \int dE\, A_E)\,(|1\rangle|E\rangle + \\ &|E\rangle|1\rangle) \\ &+ 2\,A_2 B_2\,|2\rangle|2\rangle + (A_2 \textstyle\int dE\, B_E + B_2 \int dE\, A_E)\,(|2\rangle|E\rangle + |E\rangle|2\rangle) \\ &+ \textstyle\int dE \int dE'\,(A_{E'} B_E + B_{E'} A_E)\,|E'\rangle\,|E\rangle\big]/2^{1/2}\end{aligned} \tag{3.2}$$

In order to incorporate the Pauli-exclusion principle into the dynamics, we have anti-symmetrized the two-particle state leading to

$$|\Psi_{II}(t)\rangle \equiv \left[|A(t)\rangle\,|B(t)\rangle - |B(t)\rangle\,|A(t)\rangle\right]/2^{1/2} \tag{3.3}$$

If we again express this state in terms of the same single-particle amplitudes, we obtain

$$\begin{aligned}|\Psi_{II}(t)\rangle = \big[&(A_1 B_2 - B_1 A_2)\,(|1\rangle\,|2\rangle - |2\rangle\,|1\rangle) + (A_1 \textstyle\int dE\, B_E - B_1 \int dE\, A_E)\,(|1\rangle\,|E\rangle - |E\rangle\,|1\rangle)\\ &+ (A_2 \textstyle\int dE\, B_E - B_2 \int dE\, A_E)\,(|2\rangle\,|E\rangle - |E\rangle\,|2\rangle) + \int dE' \int dE\,(A_{E'} B_E - B_{E'} A_E)\,|E'\rangle\,|E\rangle\big]/2^{1/2}\end{aligned} \tag{3.4}$$

As expected, in contrast to the decoupled system given by $|\Psi_I(t)\rangle$, here the doubly occupied states $|1\rangle\,|1\rangle$, $|2\rangle\,|2\rangle$ and $|E\rangle\,|E\rangle$ are no longer part of the dynamics as shown in Figure 1. In Appendix B we show that based on this reduced set of remaining two-particle states ($|12\rangle_-$, $|2E\rangle_-$, $|1E\rangle_-$ and $|EE'\rangle_-$), it is possible to derive a description in terms of a new effective two-level system.

The sets of the six types of time-dependent coefficients $A_1(t)$, $A_2(t)$, $A_E(t)$, $B_1(t)$, $B_2(t)$ and $B_E(t)$ are the common building blocks for both $|\Psi_I(t)\rangle$ and$|\Psi_{II}(t)\rangle$. This means we have fully analytical solutions for both states if we use the four general propagator solutions Eqs. (A.6) from Appendix A or the easier zero-detuning equations (2.4). In particular, we have $A_1(t) = U_{1,1}(t)$, $A_2(t) = U_{2,1}(t)$, $B_1(t) = U_{1,2}(t)$ and $B_2(t) = U_{2,2}(t)$.

It turns out that the dynamical impact of the Pauli exclusion principle manifests itself rather differently depending on which observable is considered. In order to compare the two dynamics described by $|\Psi_I(t)\rangle$ and $|\Psi_{II}(t)\rangle$, we will compute the time evolution of four expectation values of several multi-particle operators $P(t) = \langle\Psi(t)|\,P\,|\Psi(t)\rangle$ in the Schrödinger picture. The decomposition of the unit operator $I \otimes I$ in terms of the Hilbert space states is naturally given by nine types of direct product projections $I \otimes I = \{|1\rangle\langle 1| + |2\rangle\langle 2| + \int dE\,|E\rangle\langle E|\} \otimes \{|1\rangle\langle 1| + |2\rangle\langle 2| + \int dE\,|E\rangle\langle E|\}$. The corresponding expectation values of these nine types of product operators represent the sum of mutually excluding probabilities to find the particles in various states. Below we briefly introduce the expressions that permit us to calculate the time-dependence of the probabilities that at least one electron in state $|2\rangle$ [denoted by P(2,t)], that both electrons are bound

P(bb,t), that at least one electron is ionized P(f,t) and finally that both electrons are ionized P(ff,t). We also examine the probability to detect at least one ionized electrons inside the interval [E–ΔE/2, E+ΔE/2], denoted by P(E,t).

For example, the probability that at least one electron is in the first excited state $|2\rangle$ corresponds to the operator containing the three projections $P(2) \equiv |2\rangle\langle 2| \otimes I + I \otimes |2\rangle\langle 2| - |2\rangle\langle 2| \otimes |2\rangle\langle 2|$, where the last subtracted term is required to avoid double counting. We obtain for our two systems

$$P_I(2,t) \equiv \langle \Psi_I(t)| P(2) |\Psi_I(t)\rangle = |A_2(t)|^2 + |B_2(t)|^2 - 2|A_2(t)\, B_2(t)|^2 \quad (3.5a)$$

$$P_{II}(2,t) \equiv \langle \Psi_{II}(t)| P(2) |\Psi_{II}(t)\rangle = |A_2(t)|^2 + |B_2(t)|^2 \quad (3.5b)$$

As a side issue, we should briefly use the example of this expectation value to illustrate the impact of the indistinguishability of both particles. Had we chosen a state $|\Psi_0(t)\rangle \equiv |A(t)\rangle\, |B(t)\rangle$, where both particles are distinguishable (and also not constrained to $\langle A|B\rangle = 0$), then the resulting expectation value $\langle \Psi_0(t)| P(2) |\Psi_0(t)\rangle$ would become $P_0(2,t) = |A_2|^2 + |B_2|^2 - |A_2\, B_2|^2$. So we have the interesting result that $0 \le P_I(2,t) \le P_0(2,t) \le P_{II}(2,t) \le 1$. This means that for $\langle A|B\rangle = 0$, the symmetrization (anti-symmetrization) of a system usually decreases (increases) the probability to find at least one particle in certain state compared to that for a system of distinguishable particles. We should also remark that due to the assumed orthogonality $\langle A|B\rangle = 0$, the probabilities $|A_2(t)|^2$ and $|B_2(t)|^2$ are highly correlated with each other, such that $|A_2(t)|^2 + |B_2(t)|^2 \le 1$ at all times. Due to the different initial conditions of the underlying two single-particle systems, $P_I(2,t)$ remains positive at all times, despite the minus sign in Eq. (3.5a).

The probability that both particles are in state $|2\rangle$ is $P_I(22,t) = 2|A_2(t)\, B_2(t)|^2$ for system I and naturally vanishes for system II. This means that double occupation probability can also be found by the difference $P_I(22,t) = P_{II}(2,t) - P_I(2,t)$. We will discuss its dynamical relevance as a quantitative signature of the impact of Pauli-suppression in Section 3.

A second quantity of interest is the probability that both electrons are bound. It is associated with the operator $P(bb) \equiv |1\rangle\langle 1| \otimes |1\rangle\langle 1| + |1\rangle\langle 1| \otimes |2\rangle\langle 2| + |2\rangle\langle 2| \otimes |1\rangle\langle 1| + |2\rangle\langle 2| \otimes |2\rangle\langle 2|$. The expectation value of its complementary operator $P(f) \equiv I \otimes I - P(bb)$, would obviously correspond to the probability that at least one particle is ionized.

$$P_I(bb,t) \equiv \langle \Psi_I(t)| P(bb) |\Psi_I(t)\rangle$$

$$= 2|A_1|^2|B_1|^2 + 2|A_2|^2|B_2|^2 + |A_1|^2 |B_2|^2 + A_1^* B_1 B_2^* A_2 + B_1^* A_1 A_2^* B_2 + |A_2|^2 |B_1|^2 \quad (3.6a)$$

$$P_{II}(bb,t) \equiv \langle \Psi_{II}(t)| P(bb) |\Psi_{II}(t)\rangle$$

$$= |A_1|^2 |B_2|^2 + |A_2|^2 |B_1|^2 - A_1^* B_1 B_2^* A_2 - B_1^* A_1 A_2^* B_2 \quad (3.6b)$$

The third quantity of interest is the double ionization probability, i.e., the probability that both particles have ionized. This one is associated with the operator $P(ff) \equiv \int dE' \int dE\, |E'\rangle\langle E'| \otimes |E\rangle\langle E|$. We obtain for our two systems

$$P_I(ff,t) \equiv \langle \Psi_I(t)| P(ff) |\Psi_I(t)\rangle = (1/2) \int dE' \int dE\, |A_E B_{E'} + A_{E'} B_E|^2 \quad (3.7a)$$

$$P_{II}(ff, t) \equiv \langle \Psi_{II}(t)| P(ff) |\Psi_{II}(t)\rangle = (1/2) \int d E' \int dE\, |A_E B_{E'} - A_{E'} B_E|^2 \quad (3.7b)$$

The final quantity of interest is the probability P(E,t) to detect at least one electron in the energy interval $[E-\Delta E/2, E+\Delta E/2]$ centered around energy E with a width ΔE. It can be obtained from the expectation value $P(E,t) \equiv \langle \Psi(t)| P(E) |\Psi(t)\rangle$, where the corresponding projector is given by

$P(E) = \int_{E-\Delta E/2}^{E+\Delta E/2} dE'\, |E'\rangle\langle E'| \otimes I + I \otimes \int_{E-\Delta E/2}^{E+\Delta E/2} dE'\, |E'\rangle\langle E'| - \int_{E-\Delta E/2}^{E+\Delta E/2} dE'\, |E'\rangle\langle E'| \otimes \int_{E-\Delta E/2}^{E+\Delta E/2} dE'\, |E'\rangle\langle E'|$, where the last subtracted term avoids again the double counting. If we compute the expectation value, we obtain

$$P_I(E,t) = \int_{E-\Delta E/2}^{E+\Delta E/2} dE' |A_{E'}|^2 + \int_{E-\Delta E/2}^{E+\Delta E/2} dE'\, |B_{E'}|^2$$

$$- \int_{E-\Delta E/2}^{E+\Delta E/2} dE'\, |A_{E'}|^2 \int_{E-\Delta E/2}^{E+\Delta E/2} dE''\, |B_{E''}|^2. - \left| \int_{E-\Delta E/2}^{E+\Delta E/2} dE'\, A_{E'}^*\, B_{E'} \right|^2 \quad (3.8a)$$

$$P_{II}(E,t) = \int_{E-\Delta E/2}^{E+\Delta E/2} dE' |A_{E'}|^2 + \int_{E-\Delta E/2}^{E+\Delta E/2} dE'\, |B_{E'}|^2$$

$$- \int_{E-\Delta E/2}^{E+\Delta E/2} dE'\, |A_{E'}|^2 \int_{E-\Delta E/2}^{E+\Delta E/2} dE''\, |B_{E''}|^2 + \left| \int_{E-\Delta E/2}^{E+\Delta E/2} dE'\, A_{E'}^*\, B_{E'} \right|^2$$

$$= P_I(E,t) + 2 \left| \int_{E-\Delta E/2}^{E+\Delta E/2} dE'\, A_{E'}^*\, B_{E'} \right|^2 \quad (3.8b)$$

In the limit of $\Delta E \to \infty$, we can use the normalizations $\int_{-\infty}^{\infty} dE\ |A_E|^2 = 1 - |A_1|^2 - |A_2|^2$, $\int_{-\infty}^{\infty} dE\ |B_E|^2 = 1 - |B_1|^2 - |B_2|^2$ and the orthogonality $\int_{-\infty}^{\infty} dE\ A_E^*\ B_E = -A_1^*\ B_1 - A_2^*\ B_2$ to show that each of these two expressions simplify consistently to $P(E,t) \to P(f,t) = 1 - P(bb,t)$, where the probability $P(bb,t)$ that both electrons are bound is given by Eqs. (3.6).

In order to examine the time-dependences of P(2,t), P(f,t), P(ff,t) and P(E,t) for both systems, we have to evaluate these expressions numerically, which we perform in the next sections.

4. The impact of the Pauli exclusion principle on the ionization dynamics

In the following sections, we illustrate how the Rabi-frequency Ω_0 and the resulting possibility for resonant Rabi oscillations between the two bound states $|1\rangle$ and $|2\rangle$ will affect the ionization dynamics differently, depending on whether the Pauli-exclusion principle is present or not. We can therefore consider Ω_0 as a dynamical control field to reveal dynamical differences associated with the presence or absence of Pauli-blocking.

In particular, we will show in Section 4.1 that for the probability to find at least one electron in state $|2\rangle$ the impact of the Pauli-exclusion principle is only of transient nature. In Section 4.2, we examine the time-dependence of the single ionization probability and predict that the dynamical signature of the Pauli-suppression is the removal of the original Rabi-frequency dependence of the ionization rate, which characterizes the corresponding dynamics of the underlying single electron system. In Sections 4.3 and 4.4, we predict that -quite unexpectedly at first- the Pauli-suppression *increases* the single ionization probability, while it *decreases* the probability for double ionization. In Section 4.5, we show that the Pauli-exclusion principle manifests itself in the energy distribution of the ionized electrons, but only if the energy accumulation range of the electronic detector is chosen to be sufficiently wide.

4.1 The probability to detect at least one electron in state $|2\rangle$

We have to show first that any dynamical differences between systems I and II are solely induced by the Rabi frequency Ω_0. Therefore, we consider the special case of $\Omega_0 = 0$ first. In this limit, the ground state $|1\rangle$ is entirely decoupled from the dynamics for both systems, and we obtain $|A(t)\rangle = \mathrm{Exp}(-i\ E_1 t)\ |1\rangle$, such that $A_1(t) = \mathrm{Exp}(-i\ E_1 t)$ and $A_2(t) = A_E(t) = 0$. Similarly, in the second system we have $B_1(t) = 0$ for all times. As a consequence of the different behaviors of the

corresponding single-electron systems, the two probabilities $P_I(2,t) = P_{II}(2,t) = |B_2(t)|^2$ remain identical at all time, as one could have expected. We also obtain consistently $P_I(bb,t) = P_{II}(bb,t) = |B_2(t)|^2$, which is also identical to $1 - \int dE\, |B_E(t)|^2$, such that $P(f,t) \equiv \int dE\, |B_E(t)|^2$ and $P(ff,t) = 0$.

In order to better understand the effect due to the indistinguishability of both particles and the Pauli exclusion principle on the probability P(2,t), we first examine briefly the special but illustrative case $\gamma = 0$, where none of the two particles can ionize. As derived above in Eq. (3.5) and below, here we have simple expressions for $P_0(2,t)$, $P_I(2,t)$ and $P_{II}(2,t)$ in terms of $B_1(t)$ and $B_2(t)$. While the single-particle system probabilities $|B_1(t)|^2$ and $|B_2(t)|^2$ oscillate with period $2\pi/\Omega_0$ between $0 \le |B_i(t)|^2 \le 1$, we find that $P_0(2,t)$ and $P_I(2,t)$ oscillate doubly as fast with half that period, i.e. $2\pi/\Omega$, but with a smaller elongation, i.e., $0 \le P_0(2,t) \le 0.75$ and $0 \le P_I(2,t) \le 0.5$. One could (incorrectly) expect that the up and down transitions between states $|2\rangle$ and $|1\rangle$ could somehow cancel out, such that $P_0(2,t) = P_I(2,t)$ remains unity at all times, but this is not observed. The reason is that for both systems, the double occupation of level $|1\rangle$ is permitted dynamically, whose excitation does not contribute to P(2,t). In fact, after a quarter of the Rabi period $t_{1/4} \equiv (2\pi/\Omega_0)/4$, we have $|B_2(t)|^2 = |A_2(t)|^2 = 1/2$, leading to $P_0(2,t_{1/4}) = 0.75$ and $P_I(2,t_{1/4}) = 0.5$. Therefore, P(2,t) can decrease in time. On the other hand, for the system with Pauli suppression, the probability $P_{II}(2,t)$ remains indeed unity at all times, as any double occupation is suppressed.

After the discussion of the two special limits $\gamma = 0$ or $\Omega_0 = 0$, we will now examine the most interesting case where both γ and Ω_0 are nonzero. In Figure 3 we compare $P_I(2,t)$ with $P_{II}(2,t)$ for $\Omega_0 = 0.1$ and $\gamma = 0.15$.

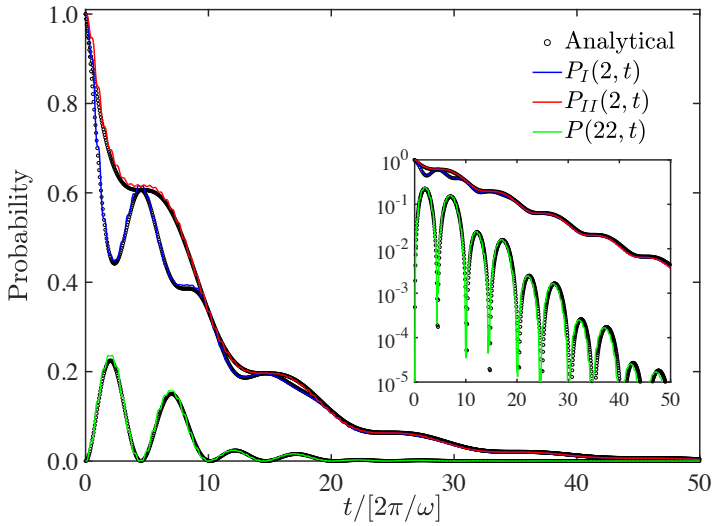

Figure 3 Comparison of the probabilities $P_I(2,t)$ and $P_{II}(2,t)$ to find at least one particle in the first excited state $|2\rangle$. Inset: Comparison of the probabilities $P_I(2,t)$ and $P_{II}(2,t)$ with the probability of double occupation $P(22,t)$ on a logarithmic scale
$\gamma = 0.15$, $\Omega_0 = 0.1$, ω=1 to $E_1 = -1.5$ and $E_2 = -0.5$.

As expected, during early times, the probability $P_I(2,t)$ decreases more rapidly than $P_{II}(2,t)$. Here in system I the electron (initially in state $|2\rangle$) has two decay channels and it is coupled to both the continuum states $|E\rangle$ as well as to level $|1\rangle$. However, the same electron in system II, cannot perform a down-ward transition to state $|1\rangle$, as this one is already occupied by the other electron and therefore this transition is blocked by the Pauli principle. As a result, it can only couple to the continuum states. We would therefore predict $P_I(2,t) \leq P_{II}(2,t)$, which is nicely confirmed by the structure of Eqs. (3.5). In fact, this equation predicts that $P_I(2,t) \leq P_{II}(2,t)$ is even valid at all times. However, it is quite astonishing that after an interaction time of about 20 optical cycles, both probabilities become graphically indistinguishable from each other, suggesting that the impact of the Pauli suppression on system II is only of transient nature.

Referring back to the Hilbert space analysis in the right of Figure 1, we remark that while an occupation all of the two-electron states $|12\rangle_+$, $|22\rangle_+$, and $|2E\rangle_+$ contribute to $P_I(2,t)$, in system II only the states $|12\rangle_-$ and $|2E\rangle_-$ contribute to $P_{II}(2,t)$. In this view of the larger space of available states, the rigid inequality $P_I(2,t) \leq P_{II}(2,t)$ for all times is not easy to be understood.

Formally, the quantitative difference between the bound state dynamics of both systems is given by the term $P(22,t) \equiv 2|A_2(t)\, B_2(t)|^2$ in Eq. (3.5a). This is proportional to the probability that the first excited state $|2\rangle$ is doubly excited. In other words, the probability that both particles

are in state $|2\rangle$ for system I is a direct measure of the dynamical impact of the Pauli suppression in system II. The transient nature of the difference between $P_I(2,t)$ and $P_{II}(2,t)$ in Figure 3 therefore suggests, that the double occupation probability should decay much more rapidly than $P_I(2,t)$ or $P_{II}(2,t)$. In the inset of Figure 3 we compare $P_I(2,t)$ and $P_{II}(2,t)$ with $P(22,t)$ on a logarithmic scale. Our conjecture that the probability $P(22,t)$ decays with an effective rate at least twice of that of either $P_I(2,t)$ or $P_{II}(2,t)$ is quite apparent. This different decay pattern is also obvious from the different functional dependence on the corresponding amplitudes of the single-particle system. For example, if we assume for simplicity that for long times the largest values of $A_2(t) \approx B_2(t)$ are given by $\mathrm{Exp}[-\Gamma t/4]$, then according to Eqs. (3.5) we have $P_I(2,t) \approx \mathrm{Exp}[-\Gamma t/2]$, while $P(22,t) \approx \mathrm{Exp}[-\Gamma t]$, so the latter decays much faster.

From a physical perspective, the transient nature of the impact of the Pauli-suppression due to the ionization channel is also apparent. At early times, the inner electron in the ground state $|1\rangle$ prohibits the outer electron in the first excited state to perform a Rabi-oscillation. However, as later times, when the total bound state probability has been reduced, the ground state is only partially occupied and therefore permits Rabi oscillations from level $|2\rangle$.

4.2 Pauli enhancement of the single ionization probability with an Ω_0 independent rate

We will next examine the impact of the Pauli principle on the time-dependence of the probability that at least one electron has ionized the atom. In order to set the stage to examine two-electron effects, we review first how a sufficiently large Rabi frequency can halve the effective ionization probability for the single electron system from the first excited state $|2\rangle$. As derived in Appendix A, in the limit of $\Omega_0 = 0$ the ionization probability $P(f,t)$ can be approximated by a simple monotonic growth $P(f,t) = 1 - \mathrm{Exp}(-\Gamma\, t)$. Here the decay constant can be derived from Fermi's Golden rule as $\Gamma \equiv 2\pi\,(\gamma/2)^2$. As Ω_0 is increased, the growth of $P(f,t)$ is halted during those moments in time, when the ground state $|1\rangle$ becomes fully excited, resulting in an overall quasi-stepwise growth of $P(f,t)$. This halt occurs precisely after odd multiples of half of the effective Rabi period, which is given by $2\pi/\Omega$. In the limit of large Ω_0, the growth returns to a simple exponential form again, but this time with an effective halved rate $\Gamma/2$, reflecting that

only half of the time the decay channel (through state $|2\rangle$) is open. We have illustrated this transition of the effective decay from Γ to $\Gamma/2$ with increasing Ω_0 in Figure 4.

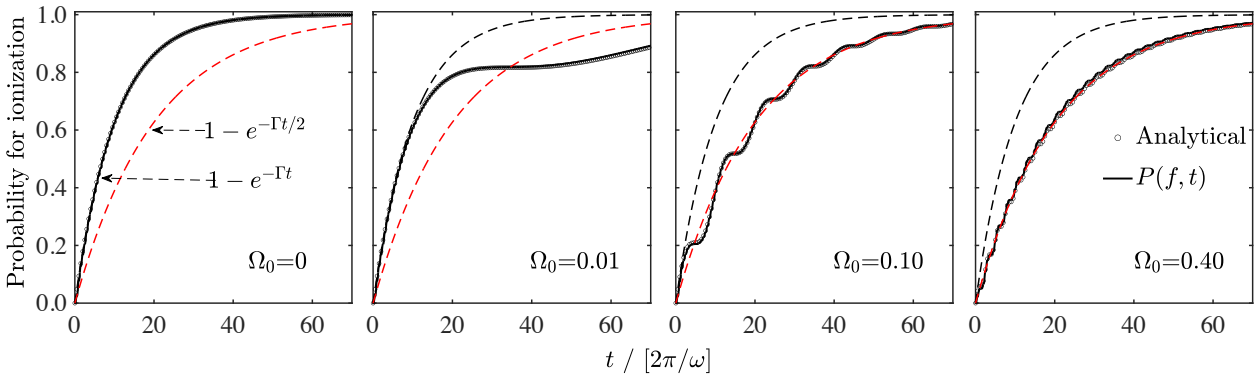

Figure 4 The ionization probability P(f,t) for the single electron system from the initial state $|2\rangle$ for four Rabi frequencies Ω_0 = 0, 0.01, 0.1 and 0.4 together with the two reference lines (dashed)
1 – Exp(– Γ t) and 1 – Exp(–Γ/2 t) for comparison. (γ = 0.1, ω=1 to E_1 =–1.5 and E_2 = –0.5)

The best curve to understand the universal behavior of all data is the one for Ω_0 = 0.01 as it provides the clearest separation of the two relevant time scales. For early times less than the Rabi period, P(f,t) follows 1 – Exp(– Γ t) until a time when the accompanying downward transition to state $|1\rangle$ has depleted level $|2\rangle$ and therefore halts the ionization. Once the first excited state gets populated again, the ionization channel opens again, but from this moment on the curve for P(f,t) oscillates around the second growth curve associated with 1 – Exp(– Γ/2 t), as the level $|2\rangle$ is populated effectively only half of the time. This universal long-time oscillatory growth pattern with a time-average given by the half-rate decay reference curve as apparent for all data for Ω_0 > 0.01.

Let us now return to the two-electron system. As is obvious from the arguments laid out above, for the special Ω_0 = 0, the Pauli suppression does not have any dynamical impact on the ionization process and we have the same ionization probabilities $P_I(f,t) = P_{II}(f,t)$, where both curves can be well approximated by 1 – Exp(– Γ t).

However, as Ω_0 is increased, the outer electron of system I can perform a downward transition. Each of the two bound-bound two-electron states $|1\rangle\,|1\rangle$ and $|2\rangle|2\rangle$ are coupled to the initial state $(|1\rangle\,|2\rangle + |2\rangle|1\rangle)/2^{1/2}$. The excitation of each of these can momentarily halt of the

ionization process after a characteristic time shown in Figure 5. At first, this observation seems to be reminiscent of the decay rate halving mechanism, which characterises the single-electron system (see Figure 4).

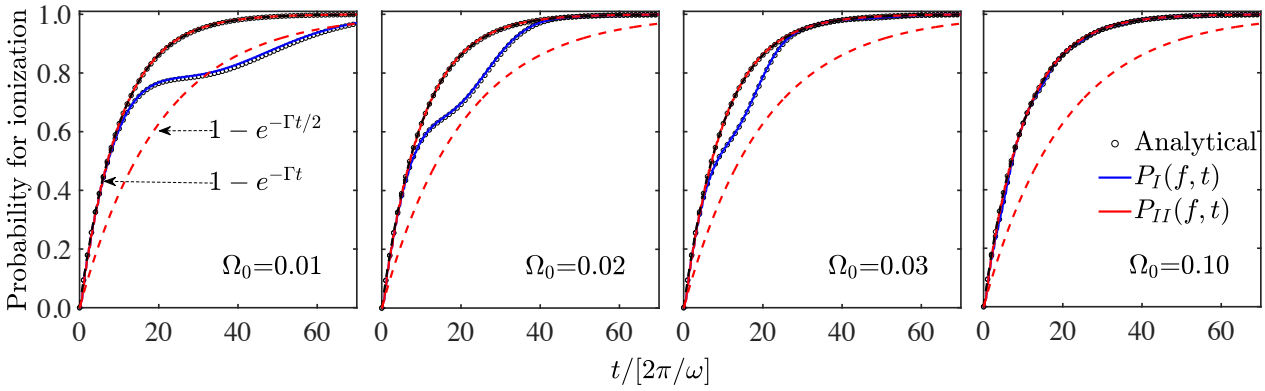

Figure 5 The probabilities $P_I(f,t)$ (blue) and $P_{II}(f,t)$ (red) to ionize at least one electron for four Rabi frequencies Ω_0 = 0, 0.01, 0.02, 0.03 and 0.1 together with the two reference lines (dashed) 1 – Exp[–Γ t] and 1 – Exp[–Γ/2 t] for comparison. (γ = 0.1, ω=1 to E_1 =–1.5 and E_2 = –0.5)

However, in contrast to the single-particle dynamics, after a longer time the probability $P_I(f,t)$ does *not* oscillate around the growth curve 1 – Exp(– Γ/2 t), but returns back to the faster decaying curve 1 – Exp(– Γ t). The explanation for this contrasting behavior is fully consistent with the discussion in Section 4.1 for $P_I(2,t)$ and $P_{II}(2,t)$. The return to 1 – Exp(– Γ t) is again related to the fact that the life time of the two doubly excited states $|1\rangle\,|1\rangle$ and $|2\rangle|2\rangle$ is much shorter than that of the state $(|1\rangle\,|2\rangle + |2\rangle|1\rangle)/2^{1/2}$. Therefore, in the limit of large Ω_0, the ionization probability $P_I(f,t)$ becomes identical to the one for vanishing Ω_0.

On the other hand, the data for system II suggest the universal and non-oscillatory growth $P_{II}(f,t) = 1 - \mathrm{Exp}(-\Gamma t)$ for *any* time and *any* Ω_0. This means that, for the entire range of Rabi-frequencies, the Pauli-exclusion principle makes the dynamics completely immune to any reduction of the ionization decay channel due to Rabi oscillations. Quite interestingly, this means that the dynamical signature of the Pauli-suppression manifests itself by the *removal* of the original Rabi-frequency *dependence* of the ionization rate, which was characteristic of the single electron dynamics.

The observed complete independence of $P_{II}(f,t)$ on any Ω_0 can also be easily understood from the perspective of the available Hilbert space states for $|\Psi_{II}(t)\rangle$. In Eq. (3.4) we saw that the initial

state $(|1\rangle|2\rangle - |2\rangle|1\rangle)/2^{1/2}$ can only couple to those states for which at least one electron is in state $|E\rangle$ and therefore ionized. This leads also to an effective modeling of the dynamics for system II as we outline in Appendix B.

4.3 Pauli suppression of the double ionization probability with an Ω_0-dependent rate

We have also compared the double ionization probabilities $P_I(ff,t)$ and $P_{II}(ff,t)$. In contrast to the remarkably robust single ionization probability, we find here that $P_{II}(ff,t)$ does change significantly with increasing Ω_0. Both $P_I(ff,t)$ and $P_{II}(ff,t)$ vanish identically in the limit of $\Omega_0 = 0$. This should be obvious as in this limit the inner electron is trapped and $A_E(t) = 0$ in Eqs. (3.7). This also means that the Rabi frequency acts as the main enabler for the possibility of double ionization.

This is shown in Figure 6. For small Ω_0 (= 0.02) the early growth of the probability $P_{II}(ff,t)$ is delayed relative to $P_I(ff,t)$, as the inner electron is initially Pauli-blocked from the upward transition. However, after a time of about 40 laser cycles the probability has caught up when its probabilty for double ionization reaches 60%. We also note that the Pauli-exclusion principle is dynamically relevant only for smaller values of the Rabi-frequency and only for early times.

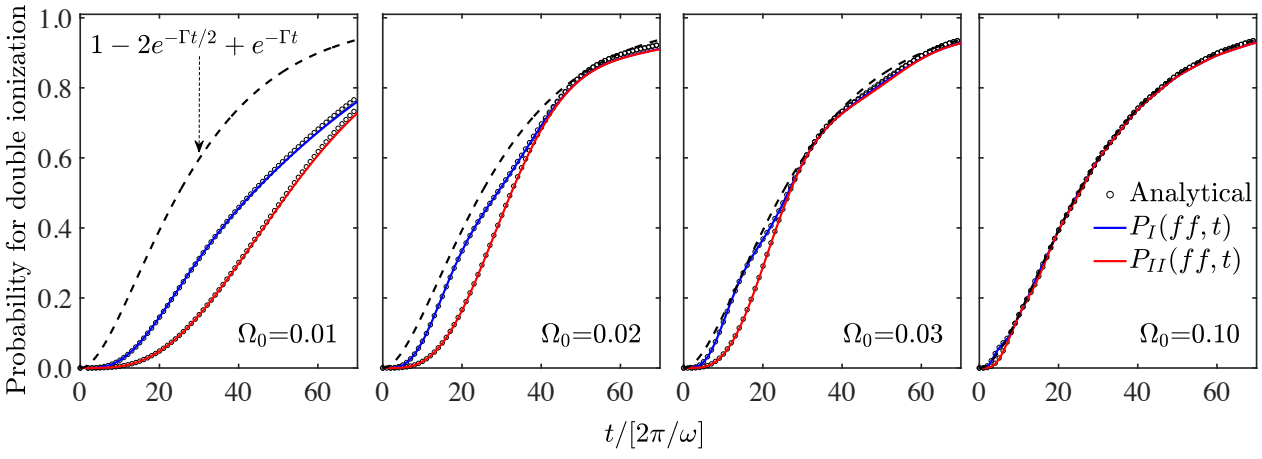

Figure 6 The double ionization probabilities $P_I(ff,t)$ and $P_{II}(ff,t)$ for four Rabi frequencies Ω_0 = 0.01, 0.02, 0.03 and 0.1 together with the reference line 1 – 2 Exp[–Γ t/2] + Exp[–Γ t] for comparison. ($\gamma = 0.1$, ω=1 to E_1 =–1.5 and E_2 = –0.5)

We note that in direct contrast to the relationship between $P_I(f,t)$ and $P_{II}(f,t)$, where we found that $P_I(f,t) \leq P_{II}(f,t)$, here we find here the reverse, $P_{II}(ff,t) \leq P_I(ff,t)$. This means that the Pauli exclusion principle *decreases* double ionization process, while at the same time it enhances the probability for single ionization. This decrease could be inferred from the possible couplings among the two-level states, which were sketched in the right Figure 1. While the initial state and $|12\rangle_-$ has only a single unique pathway to reach the doubly excited continuum states $|E'E\rangle_-$ via the states $|1E\rangle_-$, the initial state $|12\rangle_+$ can excite this continuum $|E'E\rangle_+$ via two routes. In addition to involving the states $|1E\rangle_+$ it has also an alternative route involving the intermediate states $|22\rangle_+$. On the other hand, level $|12\rangle_+$ is also coupled to state $|11\rangle_+$, which is energetically very far apart from $|E'E\rangle_+$. So it remains difficult to find an easy and intuitive explanation for the observed inequality $P_{II}(ff,t) \leq P_I(ff,t)$.

For $\Omega_0 > 0.1$, the data for $P_I(ff,t)$ and $P_{II}(ff,t)$ become graphically indistinguishable from each other. Furthermore, in the limit of large Ω_0, the probabilities become independent of Ω_0 and take the universal form $P_I(ff,t) = P_{II}(ff,t) = [1 - \mathrm{Exp}(-\Gamma t/2)]^2$. This particular expression can be easily interpreted as the double ionization probability is equal to the product of the probabilities that no electron is in state $|1\rangle$ and that no electron is in state for $|2\rangle$. In the limit of large Ω_0, the two probabilities to find at least one electron in $|1\rangle$ (and $|2\rangle$, respectively) are identical $P(1,t) \approx P(2,t) \approx \mathrm{Exp}(-\Gamma t/2)$.

The expression $P_I(ff,t) = P_{II}(ff,t) = 1 - 2\,\mathrm{Exp}(-\Gamma t/2) + \mathrm{Exp}(-\Gamma t)$ grows only quadratically for early times $P(ff,t) \approx (\Gamma^2/4)\, t^2$. This delay reflects the sequential nature of the required two consecutive ionization steps. In the opposite long-time limit, $P(ff,t)$ grows on the time-scale given by the half-decay rate $\Gamma/2$, as one might expect due to the large Rabi frequency from the two decoupled single-particle systems (see the discussion in Sec. 4.2).

4.4 The ionized electron spectra and the role of the detector's resolution

In the prior sections we found that the Pauli-suppression had only a transient impact on the dynamics and its effect decreased with increasing Rabi frequency. In this section, we will examine if the transient effect of the Pauli-suppression can actually lead to a more permanent signature with regard to the energy distribution of the ionized electrons. After the ionization is

completed, final spectra can sometimes provide features associated with the entire historical record of the evolution.

It is well known that for the single-particle system the usual single Lorentzian-shaped peak of photo-electron spectrum centered at energy $E = E_2 + \omega$ and width Γ can be split into two peaks at locations $E = E_2 + \omega \pm \Omega_0/2$. This Autler-Townes splitting can be easily understood in terms of the two dressed bound states, defined as the eigen vectors of the 2×2 interaction Hamiltonian matrix in the subspace of the bound Hilbert states. In the rotating frame, it has two dressed states with eigenvalues $E_\pm = \pm [\Omega_0^2+\Delta^2]^{1/2}/2$, where each is coupled to one group of continuum states.

In Eqs. (3.8) we have derived the formal expressions for the probability P(E,t) that at least one electron has ionized into the energy interval $[E-\Delta E/2, E+\Delta E/2]$ with an accumulation range ΔE. The similar structure of these equations for the states $|\Psi_I(t)\rangle$, and $|\Psi_{II}(t)\rangle$ reveals the inequality $P_I(E,t) \le P_{II}(E,t)$ for all times. This is interesting as it reveals that the Pauli-exclusion principle enhances the probability to detect at least one electron inside any energy range. This is consistent with the prior finding, where we predicted that the Pauli-exclusion principle would destabilize the atom favoring a more rapid ionization, i.e. $P_I(f,t) \le P_{II}(f,t)$. In fact, as we argued above, for large accumulation ranges, we have $\lim_{\Delta E\to\infty} P_I(E,t) = P_I(f,t)$ and $\lim_{\Delta E\to\infty} P_{II}(E,t) = P_{II}(f,t)$.

If we extend the energy width ΔE to ∞ and assume sufficiently long times such that both electrons are ionized, i.e. $A_1 = A_2 = B_1 = B_2 = 0$, we can use the normalization condition $\int_{-\infty}^{\infty} dE\ |A_E(t\to\infty)|^2 = \int_{-\infty}^{\infty} dE\ |B_E(t\to\infty)|^2 = 1$ as well as the orthogonality $\langle A|B\rangle = \int_{-\infty}^{\infty} dE'\ A_E(t\to\infty)^* B_E(t\to\infty) = 0$. In this case, we obtain $P_I(E, t\to\infty) = P_{II}(E, t\to\infty) = 1$.

In the opposite limit, if we assume that the energy width ΔE is much smaller than the energy variation of the amplitudes A_E and B_E, we can approximate the integrals $\int_{E-\Delta E/2}^{E+\Delta E/2} dE'\ |A_{E'}|^2 = |A_E|^2\ \Delta E + O(\Delta E^3)$ and similarly for $B_{E'}$ to obtain the simpler form

$$P_I(E,t) = \left(|A_E|^2 + |B_E|^2\right) \Delta E - 2\,|A_E|^2\,|B_E|^2\,\Delta E^2 + O(\Delta E^3) \qquad (4.1a)$$

$$P_{II}(E,t) = \left(|A_E|^2 + |B_E|^2\right) \Delta E + O(\Delta E^3) \qquad (4.1b)$$

This is very interesting as it predicts that for sufficiently small energy intervals ΔE the dynamical impact of the Pauli-principle vanishes completely, i.e., $\lim_{\Delta E\to 0} P_I(E,t) = \lim_{\Delta E\to 0} P_{II}(E,t)$.

We might note that the simultaneous scaling of $P_I(E,t)$ and $P_{II}(E,t)$ with ΔE and higher powers in ΔE is not so unusual for multi-particle probabilities. For example, for two uncorrelated random variables E_1 and E_2 that are both uniformly distributed inside [0,1], the probability to find at least one variable inside the interval $[E-\Delta E/2, E+\Delta E/2]$ (for $\Delta E/2 < E < 1 - \Delta E/2$) is given by $2\,\Delta E - \Delta E^2$, which also reflects different powers in ΔE.

Equations (4.1) have also a direct classical mechanical analogue in the long-time limit when both electrons are ionized. Let us assume the two-particle energy probability density is described by a general symmetric and continuous function $\rho(E_1, E_2) = \rho(E_2, E_1)$ and $\rho(E) \equiv \int dE_2\, \rho(E,E_2)$ denotes the corresponding marginal density. Then the probability to detect at least one electron with energy inside the interval $[E-\Delta E/2, E+\Delta E/2]$ is given by

$$P(E,\Delta E) \;=\; 2\int_{E-\Delta E/2}^{E+\Delta E/2} dE'\, \rho(E') \;-\int_{E-\Delta E/2}^{E+\Delta E/2}\int_{E-\Delta E/2}^{E+\Delta E/2} dE'\, dE''\, \rho(E',E'') \qquad (4.2)$$

If we apply the Taylor expansion around $\Delta E = 0$ together with the Leipzig product rule we obtain for small ΔE

$$P(E,\Delta E) \;=\; 2\,\rho(E)\,\Delta E \;-\; \rho(E,E)\,\Delta E^2 \;+\; O(\Delta E^3) \qquad (4.3)$$

This general expression has a remarkably similar structure as Eqs. (4.1a). This means that for small energy accumulation ranges ΔE the probabilities $P(E,\Delta E)$ for any classical (possibly highly correlated) two-particle systems [that share the same marginal density $\rho(E)$] will differ by the same Pauli-term $\rho(E,E)\,\Delta E^2$ as predicted in Eq. (4.1). Furthermore, the formal similarity permits us also to associate $(|A_E|^2+|B_E|^2)/2$ with the (identical!) marginal energy density $\rho(E)$ for systems I and II and $2|A_E|^2|B_E|^2$ with the diagonal element of the joint energy density for system I in the long-time limit.

In order to examine how the Pauli-principle affects the energy spectra more quantitatively, we have to examine the dynamics for specific parameters. In Figure 7 we compare the photo-electron

spectra $P_I(E,t)$ and $P_{II}(E,t)$ at various stages of the evolution for the two energy accumulation ranges $\Delta E=0.001$ and $\Delta E=0.02$.

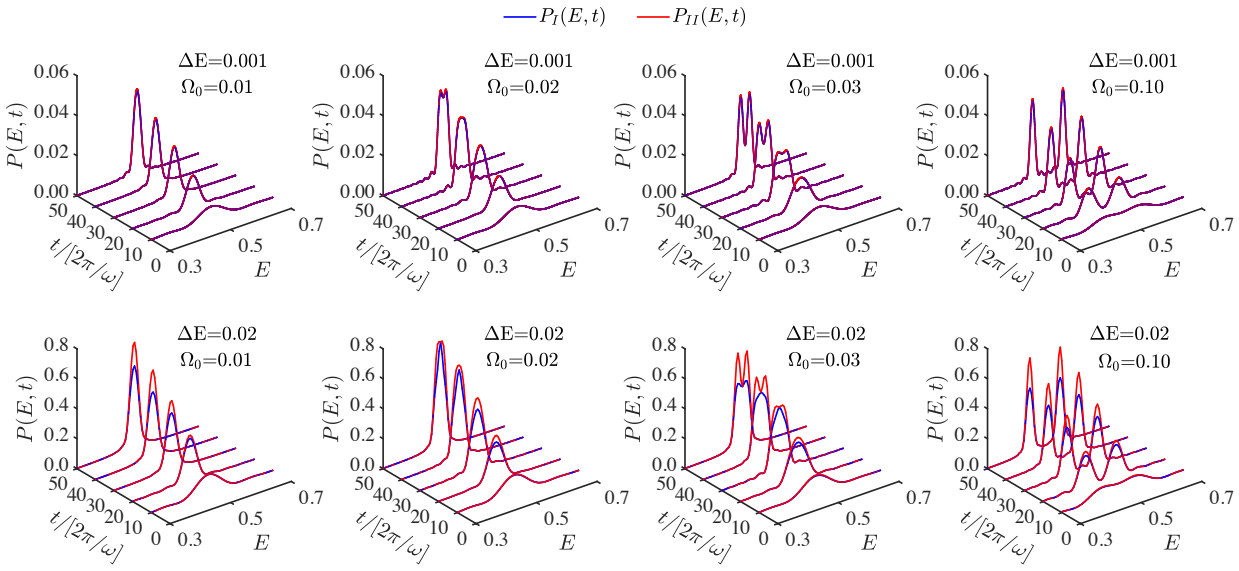

Figure 7 Comparison of the time-evolution of the photo-electron energy spectra $P_I(E,t)$ (blue) and $P_{II}(E,t)$ (red) for different Rabi frequencies Ω_0 and a small (top) and wider (bottom) energy accumulation range ΔE. All energies are in atomic units. ($\gamma = 0.1$, $\omega = 1$ to $E_1 = -1.5$ and $E_2 = -0.5$)

There are several observations with regard to the impact of the Pauli principle on the spectra as function of time, Ω_0 and ΔE. For spectra recorded by the high-resolution detector (top row in Fig. 7) we observe $P_I(E,t) \approx P_{II}(E,t)$ and therefore no impact of the Pauli principle, which is, of course, consistent with Eqs. (4.1). For the detectors with less resolution (bottom row), we find that at early times the spectra $P_I(E,t)$ and $P_{II}(E,t)$ are identical whereas at later times they begin to differ. Most importantly, in direct contrast to the ionization probabilities (see Figure 5), for which any contrast between $P_I(f,t)$ and $P_{II}(f,t)$ is only of transient nature, we observe here that the differences between $P_I(E,t)$ and $P_{II}(E,t)$ prevail for long times. This means that the Pauli-exclusion principle leads to a permanent signature manifest in the final energy distribution of the ionized electrons, if the detector's energy resolution is not too fine.

Finally, we examine if there exits an optimum accumulation range ΔE_{opt} for which the differences between the two spectra $P_I(E,t)$ and $P_{II}(E,t)$ are most significant. Returning to the simplest possible system of two uniformly distributed energies given by $\rho_I(E_1,E_2) = 1$ for $0 < E_1 <$

1 and $0 < E_2 < 1$, we can compare the spectra $P_I(E)$ with a distribution $\rho_I(E_1,E_2) = N\, \rho_I(E_1,E_2)\, H(E_1–E_2)$, where the additional Pauli-suppression function $H(E_1–E_2) \equiv 1–\mathrm{Exp}(–(E_1–E_2)^2/(2w^2))$ lowers the likelihood of two matching energies. Here N is the normalization factor and w models the energetic range on which the Pauli suppression can act. We found that independent of this "hole width" w, the largest differences $P_{II}(E) – P_I(E)$ occur for the optimum accumulation range $\Delta E \approx 0.5$, which is proportional to the total energy range covered by E_1 and E_2.

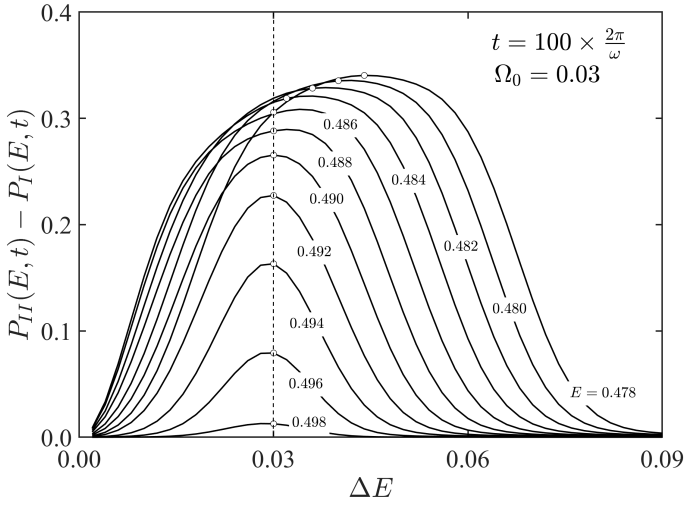

Figure 8 The difference between the final photo-electron energy spectra $P_{II}(E,t) – P_I(E,t)$ for $\Omega_0 = 0.03$ and various energies E at time $t = 100\times 2\pi/\omega$ as a function of the accumulation range ΔE. The locations of the maxima are indicated by the open circles. All energies are in atomic units. ($\gamma = 0.1$, $\omega = 1$ to $E_1 = –1.5$ and $E_2 = –0.5$)

In order to examine the same idea for our actual dynamical system, we have graphed in Figure 8 the difference $P_{II}(E,t) – P_I(E,t)$ at time $t = 100\times 2\pi/\omega$ for several central detector energies E as a function of ΔE. If the central energy E is located between the two energy peaks, i.e., $(E_2 + \omega) – \Omega_0/2 \le E \le (E_2 + \omega) + \Omega_0/2$, then it turns out that the optimal ΔE to maximize the visability of the Pauli-principle does not depend on the energy E at all. It occurs precisely at $\Delta E_{opt} = \Omega_0$, as we indicate by the vertical dashed line in the Figure. For energies E that are smaller than this range, i.e., $E \le (E_2 + \omega) – \Omega_0/2$ the optimum ΔE_{opt} grows slightly with decreasing detector's central energy. We found that here ΔE_{opt} seems to decrease linearly with E and can be well described by the dependence $\Delta E_{opt} = 2(E_2 + \omega)–2E$, which is even independent of Ω_0. This means that consistent with the findings above, the optimum ΔE_{opt} is close to the actual total effective energy range of the energies, which can be approximated by the peak-to-peak spacing given by Ω_0.

5. Conclusions and outlook to future work

In this work, we have shown that the Pauli-exclusion principle has a transient as well as permanent effect on the resonant multi-electron ionization dynamics. While the model system was remarkably simple, this principle's dynamical implications were surprisingly complex and, in some cases, even unexpected. Due to mutually competing mechanisms, it enhances the ionization probability, which is characterized by a rate that becomes *independent* of Ω_0, while at the same time it also decreases the probability for double ionization (with an Ω_0-*dependent* rate). It manifests itself also in the final energy distribution of the ionized electrons, but only if the accumulation range of the detector is chosen sufficiently *wide*. The fact that a detector with less energy resolution is more suited to detect any spectral implications of the Pauli-exclusion principle is possibly the most unexpected result. This is rather counter-intuitive at first, as one normally would have expected a better discrimination for those detectors that have the highest energy resolution. In fact, the spectral implications of the Pauli-principle are largest, if the detector covers the energy spacing of the two Autler-Townes peaks.

In order to be able to focus on the key dynamical differences due to the transient Pauli suppression of certain transitions, we have purposely chosen a model with minimal complexity with regard to the energy structure, the couplings and also the field configuration. There were two benefits, it allowed for an unambiguous comparison and also analytical solutions for any time-dependent observables to be obtained.

The simplicity of our model was facilitated by the fact that we neglected any possible energy level shifts due to electron-electron correlations and excluded possible bound state degeneracies as well as off-resonant states. Furthermore, the coupling strength to the continuum state was chosen independently of the final energy and we examined a cw-monochromatic laser field whose frequency matched exactly the bound-bound state resonance. If the intensity of the resonant laser field is chosen sufficiently large, then the magnitude of the laser induced energy shifts are significantly larger than the energy shifts (which we neglect in our model) due to electron-electron correlations, even if two electrons happen to share similar energy levels. For example, in our case the ratio of the original bare energy spacing to the laser induced Autler-Townes splitting can serve as a quantitative measure of the relative importance of the laser-dressing. For the data of most Figures, this ratio $\Omega_0/(E_2-E_1)$ amounts to 10%, which, for typical atoms or molecules, is larger than the corresponding corrections to the bare energies due to spin, relativistic or electron

correlation effects, even when the electrons happen to share the same energy level. We note that each of the two-electron energies in the effective description in Eqs. (B.3) has enough flexibility that they can easily incorporate these atomic level shifts.

As in a real atom the Pauli-exclusion principle cannot be directly turned on and off, as we did with our two-electron model systems, a corresponding experimental comparison would be more involved and requires more degrees of freedom. For example, the system could be realized in excited two-electron atoms/ions like He(1s,2p). When the 1s ground-state electron and the 2p excited electron couple their spins to a singlet (antiparallel spins), then the spatial wavefunction is symmetric and no Pauli blocking occurs. Conversely, if a spin triplet state is formed (parallel spins), the spatial wave function is antisymmetric and Pauli blocking is active. Such atoms might thus offer a natural realization of the problem under consideration.

As an example, for the possible large impact of electron-electron correlations on a realistic system, we can consider the He^+ one-electron ion, where the ground state (1s) energy is at –2 a.u., while the first excited state (2p) is at –0.5 a.u. In the absence of any correlations, the combined He 1s2p state would therefore have the energy –2.5 a.u., while its actual correct value (–2.12 a.u.) [16] is apparently higher by 15.2% due to the positive electron-electron repulsion energy. For several studies of the photoionization from $|1s, np\rangle$ states, with spin couplings in He and helium-like atoms, see [17-20]. Instead of He atoms, other highly-charged helium-like ions such as U^{90+}could be employed, where the electron-electron correlation is of minor relevance. However, such a less correlated system is experimentally more difficult to prepare.

Due to its fundamental character, the dynamical impact of the Pauli suppression on correlated fermion systems has become an active research area. For example, in a recent PRL [21] its effect on strongly interacting continuum states was observed leading to Pauli crystals. These low-temperature structures emerge when the particles become quantum degenerate.

As we have indicated in the introduction, our main motivation for this study was the exploration of the laser induced positron-electron pair creation process in the presence of a highly charged nucleus, whose (initially unoccupied) bound states can be in resonance with the laser field. Here the dynamics is similar as modeled in this work, except that it is time-reversed, as Rabi oscillations become relevant only after the created electrons have been captured by the nuclear bound states. We expect that some of the findings of this work, can be translated directly and find their dynamical impact also on these highly relativistic interactions.

Acknowledgements Dandan Su would like to thank Dr. J. Zhang for his advice and acknowledges funding from the Institute of Physics of the Chinese Academy of Sciences for her Ph.D. research. This work has been supported by the NSF, Strategic Priority Research Program of the Chinese Academy of Sciences (grant # XDA25010000) and National Natural Science Foundation of China (grant #11827807 and 11974419).

APPENDIX A

In this appendix we discuss the approximate solution to the set of coupled equations for Eqs. (2.3). There are numerous independent approaches possible [22]. We focus here on the approach that is based on the rotating wave approximation and the dominant approximation for the continuum states.

$$i\,d\,C_1/dt = E_1\,C_1 + \Omega_0/(2i)\,[\mathrm{Exp}(i\omega t) - [\mathrm{Exp}(-i\omega t)]\,C_2 \quad (A.1a)$$

$$i\,d\,C_2/dt = E_2\,C_2 + \Omega_0/(2i)\,[\mathrm{Exp}(i\omega t) - [\mathrm{Exp}(-i\omega t)]\,C_1 + \gamma_0/(2i)\,[\mathrm{Exp}(i\omega t) - [\mathrm{Exp}(-i\omega t)]\int dE\,C_E \quad (A.1b)$$

$$i\,d\,C_E/dt = E\,C_E + \gamma/(2i)\,[\mathrm{Exp}(i\omega t) - [\mathrm{Exp}(-i\omega t)]\;C_2 \quad (A.1c)$$

If we include the new amplitudes $C_1(t) \equiv \mathrm{Exp}(-i\,E_1\,t)\,D_1(t)$, $C_2(t) \equiv \mathrm{Exp}(-i\,E_2\,t)\,D_2(t)$, $C_E(t) \equiv \mathrm{Exp}(-i\,E\,t)\,D_E(t)$, this set of equations becomes

$$i\,d\,D_1/dt = \Omega_0/(2i)\,[\mathrm{Exp}(i\omega t) - [\mathrm{Exp}(-i\omega t)]\,\mathrm{Exp}(i\,E_1\,t)\,\mathrm{Exp}(-i\,E_2\,t)\,D_2(t) \quad (A.2a)$$

$$i\,d\,D_2/dt = \Omega_0/(2i)\,[\mathrm{Exp}(i\omega t) - [\mathrm{Exp}(-i\omega t)]\,\mathrm{Exp}(i\,E_2\,t)\,\mathrm{Exp}(-i\,E_1\,t)\,D_1(t) + \gamma/(2i)\,[\mathrm{Exp}(i\omega t) - [\mathrm{Exp}(-i\omega t)]\int dE\;\mathrm{Exp}(i\,E_2\,t)\,\mathrm{Exp}(-i\,E\,t)\,D_E(t) \quad (A.2b)$$

$$i\,d\,D_E/dt = \gamma/(2i)\,[\mathrm{Exp}(i\omega t) - [\mathrm{Exp}(-i\omega t)]\,\mathrm{Exp}(i\,E\,t)\,\mathrm{Exp}(-i\,E_2\,t)\,D_2(t) \quad (A.2c)$$

If we assume that $\omega - (E - E_2) << \omega + (E - E_2)$ and the detuning $\Delta \equiv \omega - (E_2 - E_1)$ is small, we can neglect the rapidly oscillating terms (rotating wave approximation) and obtain:

$$i\,d\,D_1/dt = \Omega_0/(2i)\,\mathrm{Exp}(i\,\Delta\,t)\,D_2(t) \quad (A.3a)$$

$$i\,d\,D_2/dt = -\Omega_0/(2i)\,\mathrm{Exp}(-i\,\Delta\,t)\,D_1(t) + \gamma/(2i)\int dE\;\mathrm{Exp}(i\omega t)\,\mathrm{Exp}(-i\,[E-E_2]\,t)\,D_E(t) \quad (A.3b)$$

$$i\,d\,D_E/dt = -\gamma/(2i)\,\mathrm{Exp}(-i\omega t)]\,\mathrm{Exp}(i\,[E-E_2]t)\,D_2(t) \quad (A.3c)$$

If the introduce the new amplitudes $D_1(t) \equiv \mathrm{Exp}(i\,\Delta/2\,t)\,c_1(t)$, $D_2(t) \equiv \mathrm{Exp}(-i\,\Delta/2\,t)\,c_2(t)$ and $D_E(t) \equiv \mathrm{Exp}(-i\omega t)\,\mathrm{Exp}(i\,[E-E_2]\,t)\,\mathrm{Exp}(-i\,\Delta/2\,t)\,c(E,t)$, we obtain the final time-independent equations in the rotating wave approximation

$$i\, d\, c_1 / dt \;=\; \Delta/2\; c_1 \;+ \Omega_0/(2i)\; c_2 \qquad \text{(A.4a)}$$

$$i\, d\, c_2 / dt \;=\; -\Delta/2\; c_2 - \Omega_0/(2i)\; c_1 \;+ \gamma/(2i) \int dE\; c_E \qquad \text{(A.4b)}$$

$$i\, d\, c_E / dt \;=\; (E - E_2 - \omega - \Delta/2)\; c_E \;-\; \gamma/(2i)\; c_2 \qquad \text{(A.4c)}$$

At this stage we apply the usual adiabatic approximation to the continuum amplitudes, i.e. we assume $i\, d\, c_E / dt = 0$. This means we can solve for $c_E = c_2\, \gamma/(2i) / (E - E_2 - \omega - \Delta/2)$ and insert this expression back into Eq. (4.b). We obtain

$$i\, d\, c_1 / dt \;=\; \Delta/2\; c_1 \;+ \Omega_0/(2i)\; c_2 \qquad \text{(A.5a)}$$

$$i\, d\, c_2 / dt \;=\; -\Delta/2\; c_2 - \Omega_0/(2i)\; c_1 \;- c_2\, i\, \Gamma/2 \qquad \text{(A.5b)}$$

where the simplified the integral $-c_2(\gamma^2/4) \int dE\; 1/(E - E_2 - \omega - \Delta/2)$ is equal to $-\, c_2\, i\, \Gamma/2$, where we used $\int dE\; (E - E_2 - \omega - \Delta/2)^{-1} = i\, \pi$. This means the (Fermi Golden rule) decay constant can be derived as $\Gamma \equiv 2\pi\, (\gamma/2)^2$.

The time-evolution operator $\mathrm{Exp}[-i\, H\, t]$ such that $\{c_1(t), c_2(t)\} \;=\; \mathrm{Exp}[-i\, H\, t]\; \{c_1(0), c_2(0)\}$ can be easily obtained analytically. Using abbreviation for the complex parameter $\Theta \equiv [\, (\Gamma - 2i\Delta)^2 - 4\, \Omega_0^2]^{1/2}$, we obtain for the four matrix elements

$$U_{1,1}(t) = \mathrm{Exp}[-(\Gamma+\Theta)\, t/4]\; /(2\Theta)\; [\; \Gamma\; \mathrm{Exp}(\Theta\, t/2) - \Gamma + 2\, i\, \Delta + \Theta + \mathrm{Exp}(\Theta\, t/2)\; (\Theta - 2i\Delta)] \qquad \text{(A.6a)}$$

$$U_{1,2}(t) = -\, 2\, \Omega\; \mathrm{Exp}[-\Gamma\, t/4]\; \mathrm{Sinh}(\Theta\, t/4)\; /\; \Theta \qquad \text{(A.6b)}$$

$$U_{2,1}(t) = -\, 2\, \Omega\; \mathrm{Exp}[-\Gamma\, t/4]\; \mathrm{Sinh}(\Theta\, t/4)\; /\; \Theta \qquad \text{(A.6c)}$$

$$U_{2,2}(t) = \mathrm{Exp}[-(\Gamma+\Theta)\, t/4]\; /(2\Theta)\; [\; -\, \Gamma\; \mathrm{Exp}(\Theta\, t/2) + \Gamma - 2\, i\, \Delta + \Theta + \mathrm{Exp}(\Theta\, t/2)\; (\Theta + 2i\Delta)] \qquad \text{(A.6d)}$$

From now on we will focus our attention to the limiting case of zero detuning, such that the four matrix elements simplify for $\Omega_0 > \Gamma/2 = \pi\, \gamma^2/4$ to

$$U_{1,1}(t) \;=\; \mathrm{Exp}(-t\, \Gamma/4)\; [\; \mathrm{Cos}(\Omega\, t/2) + \Gamma\; \mathrm{Sin}(\Omega\, t/2)/(2\Omega)\;] \qquad \text{(A.7a)}$$

$$U_{1,2}(t) = i\,\mathrm{Exp}(-t\,\Gamma/4)\,\Omega_0\,\mathrm{Sin}(\Omega\,t/2)/\Omega \quad \text{(A7.b)}$$

$$U_{2,1}(t) = i\,\mathrm{Exp}(-t\,\Gamma/4)\,\Omega_0\,\mathrm{Sin}(\Omega\,t/2)/\Omega \quad \text{(A.7c)}$$

$$U_{2,2}(t) = \mathrm{Exp}(-t\,\Gamma/4)\,[\,\mathrm{Cos}(\Omega\,t/2) - \Gamma\,\mathrm{Sin}(\Omega\,t/2)/(2\Omega)\,] \quad \text{(A.7d)}$$

where we have introduced the effective Rabi frequency $\Omega \equiv (\Omega_0^2 - (\Gamma/2)^2)^{1/2}$. For the other overdamped limit $\Omega_0 < \Gamma/2$, the expressions can be rewritten as

$$U_{1,1}(t) = \mathrm{Exp}(-t\,\Gamma/4)\,[\,\mathrm{Cosh}(\kappa\,t/2) + \Gamma\,\mathrm{Sinh}(\kappa\,t/2)/(2\kappa)\,] \quad \text{(A.8a)}$$

$$U_{1,2}(t) = i\,\mathrm{Exp}(-t\,\Gamma/4)\,\Omega_0\,\mathrm{Sinh}(\kappa\,t/2)/\kappa \quad \text{(A.8b)}$$

$$U_{2,1}(t) = i\,\mathrm{Exp}(-t\,\Gamma/4)\,\Omega_0\,\mathrm{Sinh}(\kappa\,t/2)/\kappa \quad \text{(A.8c)}$$

$$U_{2,2}(t) = \mathrm{Exp}(-t\,\Gamma/4)\,[\,\mathrm{Cosh}(\kappa\,t/2) - \Gamma\,\mathrm{Sinh}(\kappa\,t/2)/(2\kappa)\,] \quad \text{(A.8d)}$$

where $\kappa \equiv ((\Gamma/2)^2 - \Omega_0^2)^{1/2}$. In the limit $\Omega_0 << \Gamma/2$, these expressions become

$$U_{1,1}(t) = \mathrm{Exp}(-t\,\Gamma/4)\,[\,\mathrm{Cosh}(\kappa\,t/2) + \Gamma\,\mathrm{Sinh}(\kappa\,t/2)/(2\kappa)\,] \quad \text{(A.9a)}$$

$$U_{1,2}(t) = i\,\mathrm{Exp}(-t\,\Gamma/4)\,\Omega_0\,\mathrm{Sinh}(\kappa\,t/2)/\kappa \quad \text{(A.9b)}$$

$$U_{2,1}(t) = i\,\mathrm{Exp}(-t\,\Gamma/4)\,\Omega_0\,\mathrm{Sinh}(\kappa\,t/2)/\kappa \quad \text{(A.9c)}$$

$$U_{2,2}(t) = \mathrm{Exp}(-t\,\Gamma/4)\,[\,\mathrm{Cosh}(\kappa\,t/2) - \Gamma\,\mathrm{Sinh}(\kappa\,t/2)/(2\kappa)\,] \quad \text{(A.9d)}$$

This means, for the A system, where $\{c_1(0), c_2(0)\} = \{1,0\}$, we have $A_1(t) = U_{1,1}(t)$, $A_2(t) = U_{2,1}(t)$ and $\Sigma_E\,|A_E(t)|^2 = 1 - |U_{1,1}(t)|^2 - |U_{2,1}(t)|^2$. Similarly, for the B system, where $\{c_1(0), c_2(0)\} = \{0,1\}$, we have $B_1(t) = U_{1,1}(t)$, $B_2(t) = U_{2,1}(t)$ and $\Sigma_E\,|B_E(t)|^2 = 1 - |U_{1,2}(t)|^2 - |U_{2,2}(t)|^2$.

APPENDIX B

The focus of the discussion in the main text is to establish the dynamical impact of the Pauli-exclusion principle. To be able to compare two systems I and II requires a theoretical framework that was based on the underlying single-electron systems given by $|A(t)\rangle$ and $|B(t)\rangle$.

Due to the restricted two-particle Hilbert space for system II, it is also possible to derive a more efficient but formally identical description for this system, which we summarize here. It has also the advantage, that it can provide us with a more intuitive understanding of its predicted dynamical features. This minimal set is given by the two-electron wave function

$$|\Psi(t)\rangle = C_{12}(t)\,|1,2\rangle + \int dE\, C_{1E}(t)\,|1,E\rangle + \int dE\, C_{2E}(t)\,|2,E\rangle + \int dE' \int dE\, C_{EE'}(t)\,|E,E'\rangle \qquad (B.1)$$

where the notation such as $|1,2\rangle$ represents the antisymmetrized states. These are coupled by the effective Hamiltonian $H_0 + H_{int}$ with

$$H_0 = (E_1 + E_2)\,|1,2\rangle\langle 1,2| + \int dE\,(E_1 + E)\,|1,E\rangle\langle 1,E| + \int dE\,(E_2 + E)\,|2,E\rangle\langle 2,E| + \\ + \int dE' \int dE\,(E + E')\,|E,E'\rangle\langle E,E'| \qquad (B.2a)$$

$$H_{int} = \gamma(t) \int dE\,|1,E\rangle\langle 1,2| + \Omega(t) \int dE\,|2,E\rangle\langle 1,E| + \gamma(t) \int dE' \int dE\,|E',E\rangle\langle 2,E| + \text{h.c.} \qquad (B.2b)$$

In order to find the equation of motion of the four types of expansion coefficients $C_{12}(t)$, $C_{1E}(t)$, $C_{2E}(t)$ and $C_{EE'}(t)$, we insert the expansion for $|\Psi(t)\rangle$ into the Schrödinger equation, given by $i\,d/dt\,|\Psi\rangle = (H_0 + H_{int})\,|\Psi\rangle$. If we use the orthogonality among all states, we obtain

$$i\,d\,C_{12}/dt = (E_1+E_2)\,C_{12} + \gamma(t) \int dE\,C_{1E} \qquad (B.3a)$$

$$i\,d\,C_{1E}/dt = (E_1+E)\,C_{1E} + \gamma(t)\,C_{12} + \Omega(t)\,C_{2E} \qquad (B.3b)$$

$$i\,d\,C_{2E}/dt = (E_2+E)\,C_{2E} + \Omega(t)\,C_{1E} + \gamma(t) \int dE'\,C_{E'E} \qquad (B.3c)$$

$$i\,d\,C_{E'E}/dt = (E'+E)\,C_{E'E} + \gamma(t)\,C_{2E} \qquad (B.3d)$$

Similarly to the discussion in Appendix A, we can again eliminate approximately the faster time scales and obtain in the rotating frame a new set of equations, which no longer have an explicit

time-dependence. If we introduce the new sets of amplitudes $C_{12} \equiv c_{12}$, $C_{1E} \equiv \mathrm{Exp}(-i\omega t)\, c_{1E}$, $C_{2E} \equiv \mathrm{Exp}(-i2\omega t)\, c_{2E}$ and $C_{E'E} \equiv \mathrm{Exp}(-i3\omega t)\, c_{E'E}$ after the rotating wave approximation we obtain

$$i\, d\, c_{12}/dt = (E_1+E_2)\, c_{12} + \gamma/(2i) \int dE\, c_{2E} \tag{B.4a}$$

$$i\, d\, c_{1E}/dt = (E_1+E-\omega)\, c_{1E} + \Omega_0/(2i)\, c_{2E} - \gamma/(2i)\, c_{12} \tag{B.4b}$$

$$i\, d\, c_{2E}/dt = (E_2+E-2\omega)\, c_{2E} - \Omega_0/(2i)\, c_{1E} + \gamma/(2i) \int dE'\, c_{E'E} \tag{B.4c}$$

$$i\, d\, c_{E'E}/dt = (E+E'-3\omega)\, c_{E'E} - \gamma/(2i)\, c_{2E} \tag{B.4d}$$

This set of equations suggests the following two-electron picture based on a sequential coupling of a four-step ladder-like system comprised of one discrete and three sets of continuum states. The initial ground state $|1,2\rangle$ can decay into the first continuum $|1,E\rangle$ with coupling strength γ. The first continuum $|1,E\rangle$ is then Rabi-coupled to the second continuum $|2,E\rangle$, which is then can decay again into the third continuum $|E,E'\rangle$. The absence of Ω_0 in Eq. (B.4a) also directly supports the finding discussed in the main text that the probability $|c_{12}|^2$ decays basically monotonic and independently of Ω_0.

In fact, the easy structure of these equations permits also an access to an analytical solution under some additional simplifying approximations. We can adiabatically eliminate the sets of states $|1,2\rangle$ as well as $|E,E'\rangle$. As a first step, if we put the time derivative in Eq. (B4.b) equal to zero, we can solve for $c_{1E} = -\Omega_0/(2i)\, c_{2E}\, (E_1+E-\omega)^{-1} + \gamma/(2i)\, (E_1+E-\omega)^{-1}\, c_{12}$. As an additional approximation, we neglect the Ω_0-dependent term, such that we obtain $c_{1E} = \gamma/(2i)\, (E_1+E-\omega)^{-1}\, c_{12}$.

If we insert this expression into Eq. (B.4a), we obtain

$$i\, d\, c_{12}/dt = (E_1+E_2)\, c_{12} - i\, \Gamma/2\, c_{12} \tag{B.5}$$

where, similarly to Appendix A, we have once again assumed $\int dE\, (E_1+E-\omega)^{-1} = i\, 2\pi$, such that $\Gamma \equiv 2\pi\, (\gamma/2)^2$. The resulting equation (B.5) can be solved leading to $c_{12}(t) = \mathrm{Exp}[-i\, (E_1+E_2)t - \Gamma/2\, t\,]$.

Second, we put also the time derivative in Eq. (B.4d) equal to zero, we can solve for $c_{E'E}(t) = (E+E' -3\omega)^{-1}\, \gamma/(2i)\, c_{2E}$. If we insert the solution $c_{12}(t)$ into Eq. (B.4b) and $c_{E'E}(t)$ into Eq. (B.4c), we obtain

$$i\, d/dt\, c_{1E} = (E_1+E-\omega)\, c_{1E} + \Omega_0/(2i)\, c_{2E} - \gamma/(2i)\, Exp[-i\,(E_1+E_2)t - \Gamma\, t\,/2] \qquad (B.6a)$$

$$i\, d/dt\, c_{2E} = (E_2+E-2\omega)\, c_{2E} - \Omega_0/(2i)\, c_{1E} - i\,\Gamma/2\, c_{2E} \qquad (B.6b)$$

The structure of these two approximate equations suggests an illustrative picture of an effective discrete two-level system for the continuum amplitudes for each energy E, where the lower level is excited by an exponentially decaying source term and the upper level is exponentially damped. Note that there are no longer any energy integrals required. Due to the simple structure of these two equations, they can be solved analytically. However, the structure of these solutions is rather complicated and not very informative. Instead, we present in Figure 9 the validity of the model Eqs. (B.6) with the exact solutions for $\int dE\, |c_{1E}(t)|^2$ and $\int dE\, |c_{2E}(t)|^2$.

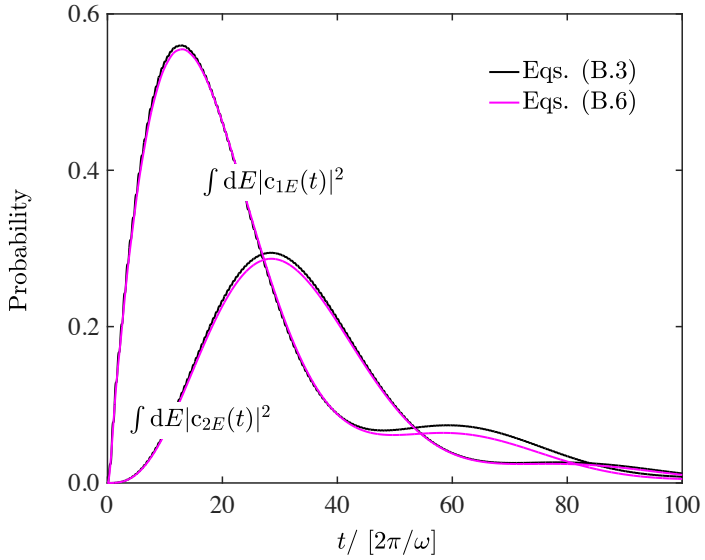

Figure 9 Comparison of the predictions for $\int dE\, |c_{1E}(t)|^2$ and $\int dE\, |c_{2E}(t)|^2$ of the approximate model Eqs. (B.6) and the exact solutions based on Eqs. (B.3). $\Omega_0 = 0.02$, $\gamma = 0.1$, $\Gamma = 0.0157$.

We see that the two sets of ionization probabilities are graphically indistinguishable, justifying the assumptions leading to Eqs. (B.6). We first see the built up of $\int dE\, |c_{1E}(t)|^2$ followed with a delayed growth of $\int dE\, |c_{2E}(t)|^2$. As the laser frequency ω $(=E_2 - E_1)$ was chosen such that the energy difference of the upper continuum and the lower continuum state, $(E_2+E-2\omega) - (E_1+E-$

ω), vanishes, the Rabi-period $2\pi/\Omega_0$ is identical for the resonant level pairs. But we do not see the periodic exchange of populations, as Γ was comparable to Ω_0.

References

[1] S.H. Autler and C.H. Townes, Phys. Rev. 100, 703 (1955).

[2] B.R. Mollow, Phys. Rev. A 5, 2217 (1972).

[3] P.L. Knight, J. Phys. B 11, L511 (1978).

[4] R. Grobe and J.H. Eberly, Phys. Rev. A 48, 623 (1993).

[5] R. Grobe and S.L. Haan, J. Phys. B 27, L735 (1994).

[6] B. Walker, M. Kaluza, B. Sheehy, P. Agostini and L.F. DiMauro, Phys. Rev. Lett. 75, 633 (1995).

[7] B. Najjari, A.B. Voitkiv, and C. Müller, Phys. Rev. Lett. 105, 153002 (2010).

[8] C. Müller and A.B. Voitkiv, Phys. Rev. Lett. 107, 013001 (2011).

[9] D.D. Su, Y.T. Li, Q. Su and R. Grobe, Phys. Rev. D 103, 074513 (2021).

[10] N. Harkema, C. Cariker, E. Lindroth, L. Argenti and A. Sandhu, Phys. Rev. Lett. 127, 023202 (2021).

[11] Z.H. Loh, C.H. Greene and S.R. Leone, Chem. Phys. 350, 7 (2008).

[12] M. Wu, S. Chen, M.B. Gaarde and K.J. Schafer, Phys. Rev. A 88, 043416 (2013).

[13] L. Argenti, Á. Jiménez-Galán, C. Marante, C. Ott, T. Pfeifer and F. Martín, Phys. Rev. A 91, 061403(R) (2015).

[14] Y. Kobayashi, H. Timmers, M. Sabbar, S.R. Leone, and D.M. Neumark, Phys. Rev. A 95, 031401 (R) (2017).

[15] N. Harkema, J.E. Baekhoj, C.-T. Liao, M.B. Gaarde, K.J. Schafer and A. Sandhu, Opt. Lett. 43, 3357 (2018).

[16] I.F. Barna and J.M. Rost, Europ. Phys. J. D, 27, 287 (2003).

[17] D. Porquet and J. Dubau, J. Astron. Astrophys. Suppl. Ser. 143, 495 (2000).

[18] I.A. Ivanov and A.S. Kheifets, Europ. Phys. J. D, 38, 471 (2006).

[19] S. Hussain, M. Saleem, M. Rafiq and M.A. Baig, Phys. Rev. A 74, 022715 (2006).

[20] V.L. Jacobs, Phys. Rev. A 9, 1938 (1974).

[21] M. Holten, L. Bayha, K. Subramanian, C. Heintze, P.M. Preiss and S. Jochim, Phys. Rev. Lett. 126, 020401 (2021).

[22] For a review, see, e.g., C.C. Gerry and P.L. Knight, "Introductory quantum optics" (Cambridge University Press, 2004, online 2012).